mathematics

MDPI

Article

New Numerical and Analytical Solutions for Nonlinear Evolution Equations Using Updated Mathematical Methods

Abdulghani R. Alharbi

Department of Mathematics, College of Science, Taibah University, Al-Madinah Al-Munawarah 42353, Saudi Arabia; arharbi@taibahu.edu.sa or abdul928@hotmail.com

Abstract: This study explores adapted mathematical methods to solve the couple-breaking soliton (BS) equations in two-dimensional spatial domains. Using these methods, we obtained analytical soliton solutions for the equations involving free parameters such as the wave number, phase component, nonlinear coefficient, and dispersion coefficient. The solutions are expressed as hyperbolic, rational, and trigonometric functions. We also examined the impact of wave phenomenon on two-dimensional diagrams and used composite two-dimensional and three-dimensional graphs to represent the solutions. We used the finite difference method to transform the proposed system into a numerical system to obtain numerical simulations for the Black–Scholes equations. Additionally, we discuss the stability and error analysis of numerical schemes. We compare the validity and accuracy of the numerical results with the exact solutions through analytical and graphical comparisons. The methodologies presented in this research can be applied to various forms of nonlinear evolutionary systems because they are appropriate and acceptable.

Keywords: BS equations; solitary solutions; numerical solutions

MSC: 65N06; 65N40; 65N45; 65N50; 35A24; 35B35; 35Q51; 35Q92

Citation: Alharbi, A.R. New Numerical and Analytical Solutions for Nonlinear Evolution Equations Using Updated Mathematical Methods. *Mathematics* **2023**, *11*, 4665. https://doi.org/10.3390/math11224665

Academic Editor: Ioannis K. Argyros

Received: 27 September 2023
Revised: 13 November 2023
Accepted: 15 November 2023
Published: 16 November 2023

1. Introduction

One of the most challenging problems in mathematical physics is the quest to find numerical and soliton solutions for the nonlinear PDEs (NPDEs). NPDEs are utilized extensively for the purpose of doing analyses on nonlinear processes. Nonlinear partial differential equations (NPDEs) have practical applications in various scientific fields. Solutions are obtained numerically and analytically using methods such as (P/Q)-expansion, Hirota bilinear, and exp-function [1–4]. In order to acquire soliton solutions for NLPDEs, a variety of approaches were utilized in order to examine the equations that were presented. The authors of [5] analyze and discuss the regularized long-wave and adjusted equal-width (MEW) equations. Wazwaz studied the KP-MEW equations using the Tanh approach in 2004. Radha and Lakshmanan examined localized structures in a pair BS equation and the Painleve property in 1995. This equation is of some assistance. In 2004, Wazwaz conducted research on the KP-MEW equations by utilizing the Tanh approach, which utilizes the (MW) equation represented in the PK purpose and is described in [6,7]. In recent decades, Radha et al. [8] researched the presence of exponentially localized systems in a (2 + 1)-dimensional pair BS equation and the Painleve property. For the two-and-a-half-dimensional plus one-dimensional BS equation, Yan and Zhang [9] created families with a solution that is analogous to a soliton. After a period of one year had passed, Chen et al. [10] utilized the recently obtained generalized expansion approach of the Riccati issue in order to achieve a soliton solution to the (2 + 1)-dimensional pair BS equation. Peng and Krishnan [11] used the singular manifold approach to examine two new kinds of exact soliton solutions for the two-and-a-half-dimensional pair BS issue. Inan [12] conducted research on the two-and-a-half-dimensional pair BS equation using the generalized Jacobi elliptic function approach. As a result of his investigation, periodic and multiple soliton solutions were obtained for the above equation. In addition to the residual symmetry that was related to the truncated Painleve expansion, Cheng et al. [13] were able to construct the nonlocal symmetry that was gained from the Lax pair. On the basis of the generalized unified technique, Osman [14] was able to obtain the multiple-soliton solutions to the two-dimensional pair BS problem. These solutions were derived for the problem. In recent years, a substantial number of researchers have examined a wide variety of analytical methodologies for the (2 + 1)-dimensional pair BS model. These researchers come from a variety of academic fields. The 2-dimensional pair BS problem has been handled by utilizing several different methodologies, such as the Hirota bilinear technique [15], the resemblance modification process [16], the cos-Gordon expansion method [17], and a few more. These many approaches have been combined in order to produce a single answer. The numerical solution to the two-dimensional fourth-order parabolic thin film equation was derived by Alharbi [18] using the parabolic Monge–Ampere approach in more recent research. Ren and Chu [19] looked at the soliton molecules and explored the generalized BS equations in two dimensions and one dimension. According to the best of our knowledge, researchers have yet to previously document in the prior literature a solution to the $(2+1)$-dimensional ZK-MEW equations and a handful of BS equations utilizing the method that is offered here. In addition, the information provided in this paper can be utilized as a supplement for other publications connected to the same overall topic area. In addition, we have begun working on a solution that incorporates hyperbolic and trigonometric function solutions with free parameters. The solutions to these issues will be extremely useful in a wide variety of sectors, including, but not limited to, scientific research, maritime engineering, and many others. In more recent research, Alharbi [18] used the parabolic Monge–Ampere technique to derive the numerical solution to the two-dimensional fourth-order parabolic thin film equation. Ren and Chu [19] investigated the generalized BS equations in two dimensions and one dimension and looked at the soliton molecules. To the best of our knowledge, researchers have yet to previously document in the literature a solution to the $(2+1)$-dimensional ZK-MEW equations and a handful of BS equations utilizing the method that is provided here. In addition, the material presented in this paper can serve as a supplement to other publications that are related to the same overarching subject area. In addition, we have started working on a solution with hyperbolic and trigonometric function solutions that incorporate free parameters. The answers to these problems will find widespread use in scientific research, maritime engineering, and a variety of other fields. The Kudryashov technique employs the transformed rational function approach [20] and the coefficient of variation for generalized breaking solitons [21]. Kaplan and Kumar [20], Kaplan and associates [22], and Kaplan and Akbulut [23] investigated the generalized Schrodinger equation, the Jaulent–Miodek equation, and fractional PDEs, respectively, all in the same year. Alharbi et al. [24] successfully found a solution to the Kadomtsev–Petviashvili problem using the adaptive moving mesh technique. Ma [25] researched nonlocally integrable NLPDEs, calculating the soliton solutions to the nonlocally integrable modified Korteweg–de Vries problem, and investigating the inverse scattering changes and soliton solutions of nonlocal integrable equations utilizing the Riemann–Hilbert problems that were made available through one-group reduction. Researchers have also discovered accurate solutions to the BS system, including double solitons and other linked forms [26], and solutions supported by trigonometry and exponential development [27]. The BS system [13,14] is considered as follows:

$$\begin{aligned} &\Gamma_t + 4\beta\Gamma\,\Psi_x + 4\beta\Gamma_x\,\Psi + \beta\,\Gamma_{xxy} = 0, \\ &\Psi_x - \Gamma_y = 0. \end{aligned} \tag{1}$$

Bogoyovlenskii [28] initially introduced this equation. Calogero and Degasperis [29,30] employed the (2 + 1)-dimensional couple BS equation to express the interaction of a Riemann wave traveling down the y-axis with a long wave traveling along the x-axis in 1996. They did this by applying the equation to the Riemann wave's matter. The wave events that are described in the equations are essential to maintaining the integrity of water wave events and maintaining tight contact. It may open the gate to further research into nonlinear wave phenomena, which are significant in the field of ocean engineering. Kazeykina and Klein [31] carried out an investigation in which they analyzed the stability of solutions for a particular equation and provided numerical solutions to the equation. In order to determine the numerical consequences of the proposed system, they also used the Kansa approach [32]. On the other hand, there has been no discussion addressing the system's stability or an error analysis of the numerical method that was used (1). Obtaining various analytic solutions to a problem (1) by utilizing modified $S-$expansion and generalized algebraic approaches was the primary purpose of this research. In order to accomplish this goal, I combined the numerical solution with finite differences in order to produce numerical results for the system that was researched. I made a substantial contribution to the comprehension of physical challenges in practice by analytically and visually comparing the solutions to traveling wave problems and the numerical outcomes of those problems. The remaining parts of this article are arranged as follows: Section 2 presents a general overview of the mathematical models. Section 3 discusses the methodology that we developed for extracting results from NLPDEs. The numerical schemes used to discover the numerical results of the proposed system (1) are presented in Section 4, together with details regarding the stability, accuracy, and convergence of those numerical schemes. After that, we derive a variety of solutions to the collection of differential equations by making use of those equations. The graphical and physical explanations of the solutions we identified will be discussed in the following section of this article. A comparison of the answers is displayed in Section 5, and the conclusion is presented in Section 6.

2. Overview of Proposed Procedures

The following form represents the development equations with the physical fields $\Gamma(x, y, t)$ and $\Psi(x, y, t)$ in the variables x, y, and t.

$$\begin{aligned} &G_1(\Gamma_t,\, \Gamma_x,\, \Gamma_y,\, \Gamma_{xxy},\, \Psi,\, \Psi_y, \Psi_x \ldots) = 0, \\ &G_2(\Psi_x,\, \Gamma_y,\, \Gamma_{xxy},\, \Psi,\, \Psi_y, \Psi_x \ldots) = 0. \end{aligned} \tag{2}$$

Step 1. We obtain the System (1) traveling-wave solutions, which are created as follows:

$$\begin{aligned} \Gamma(x, y, t) =&\Phi(\zeta), \qquad\qquad \zeta = x + y - \alpha\, t, \\ \Psi(x, y, t) =&\Theta(\zeta). \end{aligned} \tag{3}$$

where α is the wave's speed.

Step 2. The following ODE represents the nonlinear evolution (2):

$$\begin{aligned} &G_3(\Phi,\, \Phi_\zeta,\, \Phi_{\zeta\zeta\zeta},\, \Theta,\, \Theta_\zeta,\, \ldots) = 0, \\ &G_4(\Theta,\, \Theta_\zeta, \Phi,\, \Phi_\zeta,\, \ldots) = 0. \end{aligned} \tag{4}$$

where G_3 and G_4 are polynomials with respect to $\Theta(\zeta)$, $\Phi(\zeta)$, and their combined derivatives.

The generalized indirect algebraic approach suggests that the solution to (4) is

$$\Phi(\zeta) = \rho_0 + \sum_{k=1}^{N} \left(\rho_k \psi(\zeta)^k + \frac{s_k}{\psi(\zeta)^k} \right), \tag{5}$$

where $\psi(\zeta)$ is a solution of

$$\psi'(\zeta) = \left(\sum_{k=0}^{4} \gamma_k \psi^k(\zeta) \right)^{\dfrac{1}{2}}, \tag{6}$$

where ρ_k, and s_k are to be determined, and N is a positive integer that balances the highest possible degree of the nonlinear terms and the highest order of the derivatives. The relationships between γ_k and $0 \leq k \leq 4$ are listed in Table 1 [33].

Table 1. The relationships between γ_k, $0 \leq k \leq 4$, and the function $\psi(\zeta)$.

$(\gamma_0, \gamma_1, \gamma_2, \gamma_3, \gamma_4)$	$\psi(\zeta)$
$\left(\gamma_0 = \frac{\gamma_2^2}{4\gamma_4}, \gamma_1 = 0, \gamma_2 < 0, \gamma_3 = 0, \gamma_4 > 0\right)$	$\psi(\zeta) = \sqrt{-\frac{\gamma_2}{2\gamma_4}} \tanh\left(\sqrt{-\frac{\gamma_2}{2}}\zeta\right).$
$(\gamma_0 = 0, \gamma_1 = 0, \gamma_2 > 0, \gamma_3 = 0, \gamma_4 < 0)$	$\psi(\zeta) = \sqrt{-\frac{\gamma_2}{\gamma_4}} \operatorname{sech}(\sqrt{\gamma_2}\zeta).$
$\left(\gamma_0 = \frac{\gamma_2^2}{4\gamma_4}, \gamma_1 = 0, \gamma_2 > 0, \gamma_3 = 0, \gamma_4 > 0\right)$	$\psi(\zeta) = \sqrt{\frac{\gamma_2}{2\gamma_4}} \tan\left(\sqrt{\frac{\gamma_2}{2}}\zeta\right).$
$(\gamma_0 = 0, \gamma_1 = 0, \gamma_2 = 0, \gamma_3 = 0, \gamma_4 > 0,)$	$\psi(\zeta) = -\frac{1}{\sqrt{\gamma_4}\zeta}.$
$(\gamma_0 = 0, \gamma_1 = 0, \gamma_2 < 0, \gamma_3 = 0, \gamma_4 > 0)$	$\psi(\zeta) = \sqrt{-\frac{\gamma_2}{\gamma_4}} \sec(\sqrt{-\gamma_2}\zeta).$
$(\gamma_0 = 0, \gamma_1 = 0, \gamma_2 > 0, \gamma_3 \neq 0, \gamma_4 = 0)$	$\psi(\zeta) = -\frac{\gamma_2}{\gamma_3} \operatorname{sech}^2\left(\frac{\sqrt{\gamma_2}}{2}\zeta\right).$

The Modified S—the expansion method yields the following solutions to Equation (4):

$$\psi(\zeta) = \lambda_0 + \sum_{k=1}^{N} \left(\lambda_k S(\zeta)^k + \frac{q_k}{S(\zeta)^k}\right), \tag{7}$$

where $S(\zeta)$ is a solution of

$$S'(\zeta) = \mu_0 + \mu_1 S(\zeta) + \mu_2 S(\zeta)^2 \tag{8}$$

where μ_k and $0 \leq k \leq 2$ are listed in Table 2 [34] and q_k and λ_k are to be obtained later.

Table 2. The relationships between μ_k, $0 \leq k \leq 2$, and the function $S(\zeta)$.

(μ_0, μ_1, μ_2)	$S(\zeta)$
$(\mu_0 = 0.5, \mu_1 = 0.0, \mu_2 = 0.5)$	$S(\zeta) = \sec(\zeta) + \tan(\zeta), \csc(\zeta) - \cot(\zeta).$
$(\mu_0 = 0.5, \mu_1 = 0.0, \mu_2 = 0.5)$	$S(\zeta) = \sec(\zeta) - \tan(\zeta), \csc(\zeta) + \cot(\zeta).$
$(\mu_0 = \pm 1, \mu_1 = 0.0, \mu_2 = \pm 1)$	$S(\zeta) = \tan(\zeta), \cot(\zeta).$
$(\mu_0 = 0.0, \mu_1 = 1.0, \mu_2 = -1.0)$	$S(\zeta) = \frac{1}{2}\left(1 + \tanh\left(\frac{1}{2}\zeta\right)\right).$
$(\mu_0 = 1.0, \mu_1 = 0.0, \mu_2 = -1.0)$	$S(\zeta) = \tanh(\zeta), \coth(\zeta).$
$(\mu_0 = 1/2, \mu_1 = 0.0, \mu_2 = -1/2)$	$S(\zeta) = \tanh(\zeta) \pm \operatorname{sech}(\zeta), \coth(\zeta) \pm \operatorname{csch}(\zeta).$

3. Methodology

Consider the couple-breaking soliton (BS) Equation (1). By applying the appropriate transformations, the equation denoted as Equation (1) can be simplified into a system of ordinary differential equations (ODEs) in the following manner:

$$\begin{aligned} \Gamma(x, y, t) &= \Phi(\zeta), \qquad\qquad \zeta = x + y - \alpha\, t, \\ \Psi(x, y, t) &= \Theta(\zeta). \end{aligned} \tag{9}$$

As a result, Equation (1) is presented as

$$\begin{aligned} -\alpha\, \Phi_\zeta + 4\beta\Phi\, \Theta_\zeta + 4\beta\Phi_\zeta\, \Theta + \beta\, \Phi_{\zeta\zeta\zeta} &= 0, \\ \Theta_\zeta - \Phi_\zeta &= 0. \end{aligned} \tag{10}$$

Integrating the second equation in (10) with respect to ζ yields $\Theta = \Phi$. Thus, the first equation in (10) is given by

$$-\alpha\,\Phi + 4\beta\,\Phi^2 + \beta\,\Phi_{\zeta\zeta} = 0. \tag{11}$$

In (11), the value of $N = 2$ is determined by balancing $\Phi_{\zeta\zeta}$ with Φ^2.

Based on the modified $S-$expansion method with $N = 2$, the solution to (11) is

$$\psi(\zeta) = \lambda_0 + \lambda_1 S(\zeta) + \frac{q_1}{S(\zeta)} + \lambda_2 S(\zeta)^2 + \frac{q_2}{S(\zeta)^2}, \tag{12}$$

where $S(\zeta)$ is a solution of

$$F'(\zeta) = \mu_0 + \mu_1 S(\zeta) + \mu_2 S(\zeta)^2. \tag{13}$$

In addition, μ_i, $i = 0, 1, 2$, are listed in Table 2. In order to examine the analytical solutions to (11), the steps outlined below should be followed.

(1) A system of equations for λ_0, λ_m, q_m, where $m = 1, 2$, can be obtained by incorporating (12) and (13) into Equation (11) and setting all of the coefficients of $S(\zeta)^m$, $-4 \leq m \leq 4$ to zero;

(2) Mathematical software, such as Mathematica 13.2 or Maple 2023.1, should be employed to solve the resulting system;

(3) Using the values of μ_0, μ_1 and μ_2, and the function $S(\zeta)$ from Table 2, and substituting them along with λ_0, λ_k, q_k, $k = 1, 2$ into Equation (12), several trigonometric functions and rational solutions to Equation (11) are obtained.

Using the preceding steps, I determined the following values for λ_0, λ_1, λ_2, q_1, q_2, and α:

1. When $\mu_0 = 0$, $\mu_1 = \pm 1$, and $\mu_2 = \mp 1$, the solutions of System (1) Γ are provided using

$$\begin{aligned}
\Gamma_1(x,y,t) =& -\frac{1}{4} + \frac{3}{4}(1 + \tanh((x + y + \beta\,t)/2)) - \frac{3}{8}(1 + \tanh((x + y + \beta\,t)/2))^2, \\
\Psi_1(x,y,t) =& \frac{1}{8}\left(1 - 3\tanh^2\left(\frac{1}{2}(\beta t + x + y)\right)\right), \\
\Gamma_2(x,y,t) =& -\frac{1}{4} + \frac{3}{4}(1 + \coth((x + y + \beta\,t)/2))\left[1 - \frac{1}{2}(1 + \coth((x + y + \beta\,t)/2))\right], \\
\Psi_2(x,y,t) =& \frac{1}{8}\left(1 - 3\coth^2\left(\frac{1}{2}(\beta \mathrm{t} + x + y)\right)\right), \\
\Gamma_3(x,y,t) =& \frac{3}{4}(1 + \tanh((x + y - \beta\,t)/2)) - \frac{3}{8}(1 + \tanh((x + y - \beta\,t)/2))^2, \\
\Psi_3(x,y,t) =& -\frac{3}{8}\left(\tanh^2\left(\frac{1}{2}(-\beta t + x + y)\right) - 1\right), \\
\Gamma_4(x,y,t) =& \frac{3}{4}(1 + \coth((x + y + \beta\,t)/2))\left[1 - \frac{1}{2}(1 + \coth((x + y + \beta\,t)/2))\right], \\
\Psi_4(x,y,t) =& \frac{1}{8}(-3)\left(\coth^2\left(\frac{1}{2}(\beta t + x + y)\right) - 1\right).
\end{aligned} \tag{14}$$

2. When $\mu_0 = 1$, $\mu_1 = 0$, and $\mu_2 = -1$, two cases exist. The solutions are

$$
\begin{aligned}
\Gamma_5(x,y,t) =& \frac{3}{2} - \frac{3}{2}\tanh^2((x+y-4\beta\, t)),\\
\Psi_5(x,y,t) =& \frac{3}{2}\operatorname{sech}^2(-4\beta t + x + y),\\
\Gamma_6(x,y,t) =& \frac{3}{2} - \frac{3}{2}\coth^2((x+y-4\beta\, t)),\\
\Psi_6(x,y,t) =& -\frac{3}{2}\operatorname{csch}^2(-4\beta t + x + y),\\
\Gamma_7(x,y,t) =& -1 - \frac{3}{2}\Big(\tanh^2((x+y+16\beta\, t)) + \coth^2((x+y+16\beta\, t))\Big),\\
\Psi_7(x,y,t) =& -\frac{3}{2}\Big(\tanh^2(16\beta t + x + y) + \coth^2(16\beta t + x + y)\Big) - 1,\\
\Gamma_8(x,y,t) =& \frac{1}{2} - \frac{3}{2}\tanh^2(4\beta\, t + x + y),\\
\Psi_8(x,y,t) =& \frac{1}{2}\Big(1 - 3\tanh^2(4\beta t + x + y)\Big),\\
\Gamma_9(x,y,t) =& \frac{1}{2} - \frac{3}{2}\coth^2(4\beta\, t + x + y),\\
\Psi_9(x,y,t) =& \frac{1}{2}\Big(1 - 3\coth^2(4\beta t + x + y)\Big),\\
\Gamma_{10}(x,y,t) =& 3 - \frac{3}{2}\tanh^2(16\beta t - x - y) - \frac{3}{2}\coth^2(16\beta t - x - y),\\
\Psi_{10}(x,y,t) =& -6\operatorname{csch}^2(2(-16\beta \mathrm{t} + x + y)).
\end{aligned}
\tag{15}
$$

3. When $\mu_0 = \frac{1}{2}$, $\mu_1 = 0$, and $\mu_2 = \frac{1}{2}$, the solutions are

$$
\begin{aligned}
\Gamma_{11}(x,y,t) =& -\frac{3}{8}\Big(1 + (\sec(x+y+\beta\, t) \pm \tan(x+y+\beta\, t))^2\Big),\\
\Psi_{11}(x,y,t) =& -\frac{3}{8}(\sec(\beta t + x + y) \pm \tan(\beta t + x + y))^2 - \frac{3}{8}\\
\Gamma_{12}(x,y,t) =& \frac{1}{4} - \frac{3}{8}\Big((\sec(x+y+4\beta\, t) + \tan(x+y+4\beta\, t))^2 +\\
& (\sec(x+y+4\beta\, t) + \tan(x+y+4\beta\, t))^{-2}\Big),\\
\Psi_{12}(x,y,t) =& \frac{1}{8}\Big(-3(\tan(4\beta t + x + y) + \sec(4\beta t + x + y))^2\\
& - \frac{3}{(\tan(4\beta t + x + y) + \sec(4\beta t + x + y))^2} + 2\Big).
\end{aligned}
\tag{16}
$$

4. When $\mu_0 = \frac{1}{2}$, $\mu_1 = 0$, and $\mu_2 = -\frac{1}{2}$, the solutions are

$$\begin{aligned}
\Gamma_{13}(x,y,t) =& \frac{1}{8}\left(-3\tanh^2\left(\frac{1}{2}(4\beta t + x + y)\right) - 3\coth^2\left(\frac{1}{2}(4\beta t + x + y)\right) - 2\right),\\
\Psi_{13}(x,y,t) =& -\frac{3}{8}\tanh^2\left(\frac{1}{2}(4\beta\mathrm{t} + x + y)\right) - \frac{1}{8}3\coth^2\left(\frac{1}{2}(4\beta t + x + y)\right) + \frac{1}{4},\\
\Gamma_{14}(x,y,t) =& \frac{1}{8} - \frac{3}{8}(\coth(\beta t + x + y) + \operatorname{csch}(\beta t + x + y))^2,\\
\Psi_{14}(x,y,t) =& -\frac{1}{8}(\cosh(\beta t + x + y) + 2)\operatorname{csch}^2\left(\frac{1}{2}(\beta\mathrm{t} + x + y)\right),\\
\Gamma_{15}(x,y,t) =& \frac{1}{8} - \frac{3}{8}(\coth(\beta t + x + y) + \operatorname{csch}(\beta t + x + y))^{-2},\\
\Psi_{15}(x,y,t) =& \frac{1}{8}\left(1 - 3(\coth(\beta t + x + y) + \operatorname{csch}(\beta t + x + y))^{-2}\right),\\
\Gamma_{16}(x,y,t) =& \frac{1}{8}\left(1 - 3\coth^2\left(\frac{1}{2}(\beta t + x + y)\right)\right),\\
\Psi_{16}(x,y,t) =& \frac{1}{8} - \frac{3}{8}\coth^2\left(\frac{1}{2}(\beta\mathrm{t} + x + y)\right),\\
\Gamma_{17}(x,y,t) =& \frac{3}{8}\operatorname{sech}^2\left(\frac{1}{2}(\beta t - x - y)\right),\\
\Psi_{17}(x,y,t) =& \frac{3}{4}(1 + \cosh(x + y - \beta t))^{-1}.
\end{aligned} \tag{17}$$

Based on the generalized algebraic method with $N = 2$, the solution to (11) is

$$\Phi(\zeta) = \rho_0 + \rho_1\psi(\zeta) + \rho_2\psi(\zeta)^2 + \frac{s_1}{\psi(\zeta)} + \frac{s_2}{\psi(\zeta)^2}, \tag{18}$$

where $\psi(\zeta)$ is a solution of

$$\psi'(\zeta) = \sqrt{\gamma_0 + \gamma_1\psi(\zeta) + \gamma_2\psi^2(\zeta) + \gamma_3\psi^3(\zeta) + \gamma_4\psi^4(\zeta)}. \tag{19}$$

Table 1 contains a list of all possible values for γ_j, $j = 0, 1, 2, 3, 4$. To determine the values of the coefficients ρ_0, ρ_1, ρ_2, s_1, s_2, and α in all of the scenarios mentioned earlier and their subsequent solutions, I used mathematical software, specifically Mathematica 13.2, to obtain the values. As a result, the analytic solutions to Equation (13) will be shown in this section using the generalized algebraic method with various alternative values for γ_k, $k = 0, 1, 3, 4$.

4. If $\gamma_0 = 0$, $\gamma_1 = 0$, $\gamma_2 > 0$, $\gamma_3 = 0$ and $\gamma_4 < 0$, then

$$\begin{aligned}
\Gamma_{18}(x,y,t) =& \frac{3}{2}\gamma_2\operatorname{sech}^2(\sqrt{\gamma_2}(x + y - 4\beta\gamma_2 t)),\\
\Gamma_{19}(x,y,t) =& -\gamma_2 + \frac{3}{2}\gamma_2\operatorname{sech}^2(\sqrt{\gamma_2}(x + y - 4\beta\gamma_2 t)).
\end{aligned} \tag{20}$$

$$\begin{aligned}
\Psi_{18}(x,y,t) =& \frac{3}{2}\gamma_2\operatorname{sech}^2(\sqrt{\gamma_2}(x + y - 4\beta\gamma_2 t)),\\
\Psi_{19}(x,y,t) =& -\gamma_2 + \frac{3}{2}\gamma_2\operatorname{sech}^2(\sqrt{\gamma_2}(x + y - 4\beta\gamma_2 t)).
\end{aligned} \tag{21}$$

5. If $\gamma_0 = \frac{\gamma_2^2}{4\gamma_4 4}$, $\gamma_1 = 0$, $\gamma_2 < 0$, $\gamma_3 = 0$, and $\gamma_4 > 0$, then

$$\begin{aligned}
\Gamma_{20}(x,y,t) =& 3\gamma_2 \operatorname{csch}^2\left(\sqrt{2}\sqrt{-\gamma_2}(8\beta\gamma_2 t + x + y)\right), \\
\Gamma_{21}(x,y,t) =& \frac{3}{4}\gamma_2\left[\tanh^2\left(\frac{\sqrt{-\gamma_2}(2\beta\gamma_2 t + x + y)}{\sqrt{2}}\right) - 1\right], \\
\Gamma_{22}(x,y,t) =& \frac{1}{4}\gamma_2\left(3\tanh^2\left(\frac{\sqrt{-\gamma_2}(-2\beta\gamma_2 t + x + y)}{\sqrt{2}}\right) - 1\right) \\
\Gamma_{23}(x,y,t) =& \frac{3}{4}\gamma_2 \operatorname{csch}^2\left(\frac{\sqrt{-\gamma_2}(2\beta\gamma_2 t + x + y)}{\sqrt{2}}\right), \\
\Gamma_{24}(x,y,t) =& \frac{1}{4}\gamma_2\left(3\tanh^2\left(\frac{\sqrt{-\gamma_2}(-8\beta\gamma_2 t + x + y)}{\sqrt{2}}\right)\right. \\
&\left. + 3\coth^2\left(\frac{\sqrt{-\gamma_2}(-8\beta\gamma_2 t + x + y)}{\sqrt{2}}\right) + 2\right).
\end{aligned} \tag{22}$$

$$\begin{aligned}
\Psi_{20}(x,y,t) =& 3\gamma_2 \operatorname{csch}^2\left(\sqrt{2}\sqrt{-\gamma_2}(8\beta\gamma_2 t + x + y)\right), \\
\Psi_{21}(x,y,t) =& \frac{3}{4}\gamma_2\left[\tanh^2\left(\frac{\sqrt{-\gamma_2}(2\beta\gamma_2 t + x + y)}{\sqrt{2}}\right) - 1\right], \\
\Psi_{22}(x,y,t) =& \frac{1}{4}\gamma_2\left(3\tanh^2\left(\frac{\sqrt{-\gamma_2}(-2\beta\gamma_2 t + x + y)}{\sqrt{2}}\right) - 1\right) \\
\Psi_{23}(x,y,t) =& \frac{3}{4}\gamma_2 \operatorname{csch}^2\left(\frac{\sqrt{-\gamma_2}(2\beta\gamma_2 t + x + y)}{\sqrt{2}}\right), \\
\Psi_{24}(x,y,t) =& \frac{1}{4}\gamma_2\left(3\tanh^2\left(\frac{\sqrt{-\gamma_2}(-8\beta\gamma_2 t + x + y)}{\sqrt{2}}\right)\right. \\
&\left. + 3\coth^2\left(\frac{\sqrt{-\gamma_2}(-8\beta\gamma_2 t + x + y)}{\sqrt{2}}\right) + 2\right).
\end{aligned} \tag{23}$$

6. If $\gamma_0 = 0$, $\gamma_1 = 0$, $\gamma_2 > 0$, $\gamma_3 \neq 0$, and $\gamma_4 = 0$, then

$$\begin{aligned}
\Gamma_{25}(x,y,t) =& \frac{3}{8}\gamma_2 \operatorname{sech}^2\left(\frac{1}{2}\sqrt{\gamma_2}(-\beta\gamma_2 t + x + y)\right), \\
\Gamma_{26}(x,y,t) =& -\frac{\gamma_2}{4} + \frac{3}{8}\gamma_2 \operatorname{sech}^2\left(\frac{1}{2}\sqrt{\gamma_2}(\beta\gamma_2 t + x + y)\right).
\end{aligned} \tag{24}$$

$$\begin{aligned}
\Psi_{25}(x,y,t) =& \frac{3}{8}\gamma_2 \operatorname{sech}^2\left(\frac{1}{2}\sqrt{\gamma_2}(-\beta\gamma_2 t + x + y)\right), \\
\Psi_{26}(x,y,t) =& -\frac{\gamma_2}{4} + \frac{3}{8}\gamma_2 \operatorname{sech}^2\left(\frac{1}{2}\sqrt{\gamma_2}(\beta\gamma_2 t + x + y)\right).
\end{aligned} \tag{25}$$

7. If $\gamma_0 = 0$, $\gamma_1 = 0$, $\gamma_2 < 0$, $\gamma_3 = 0$, $\gamma_4 > 0$, then

$$\begin{aligned}
\Gamma_{27}(x,y,t) =& \frac{3}{2}\gamma_2 \sec^2\left(\sqrt{-\gamma_2}(-4\beta\gamma_2 t + x + y)\right), \\
\Gamma_{28}(x,y,t) =& \frac{3}{2}\gamma_2 \sec^2\left(\sqrt{-\gamma_2}(4\beta\gamma_2 t + x + y)\right) - \gamma_2.
\end{aligned} \tag{26}$$

$$\begin{aligned}
\Psi_{27}(x,y,t) =& \frac{3}{2}\gamma_2 \sec^2\left(\sqrt{-\gamma_2}(-4\beta\gamma_2 t + x + y)\right), \\
\Psi_{28}(x,y,t) =& \frac{3}{2}\gamma_2 \sec^2\left(\sqrt{-\gamma_2}(4\beta\gamma_2 t + x + y)\right) - \gamma_2.
\end{aligned} \tag{27}$$

8. If $\gamma_0 = \frac{\gamma_2^2}{4\gamma_4}$, $\gamma_1 = 0$, $\gamma_2 > 0$, $\gamma_3 = 0$, $\gamma_4 > 0$, then

$$\begin{aligned}
\Gamma_{29}(x,y,t) &= -\frac{3}{4}\gamma_2 \tan^2\left(\frac{\sqrt{\gamma_2}(8\beta\gamma_2 t + x + y)}{\sqrt{2}}\right) \\
&\quad -\frac{1}{4}3\gamma_2 \cot^2\left(\frac{\sqrt{\gamma_2}(8\beta\gamma_2 t + x + y)}{\sqrt{2}}\right) - \frac{3\gamma_2}{2}, \\
\Gamma_{30}(x,y,t) &= -\frac{1}{4}3\gamma_2 \tan^2\left(\frac{\sqrt{\gamma_2}(2\beta\gamma_2 t + x + y)}{\sqrt{2}}\right) - \frac{3\gamma_2}{4}, \\
\Gamma_{31}(x,y,t) &= -\frac{1}{4}3\gamma_2 \cot^2\left(\frac{\sqrt{\gamma_2}(2\beta\gamma_2 t + x + y)}{\sqrt{2}}\right) - \frac{3\gamma_2}{4}, \\
\Gamma_{32}(x,y,t) &= -\frac{1}{4}3\gamma_2 \tan^2\left(\frac{\sqrt{\gamma_2}(-2\beta\gamma_2 t + x + y)}{\sqrt{2}}\right) - \frac{\gamma_2}{4}, \\
\Gamma_{33}(x,y,t) &= -\frac{1}{4}3\gamma_2 \cot^2\left(\frac{\sqrt{\gamma_2}(-2\beta\gamma_2 t + x + y)}{\sqrt{2}}\right) - \frac{\gamma_2}{4},
\end{aligned} \tag{28}$$

$$\begin{aligned}
\Psi_{29}(x,y,t) &= -\frac{3}{4}\gamma_2 \tan^2\left(\frac{\sqrt{\gamma_2}(8\beta\gamma_2 t + x + y)}{\sqrt{2}}\right) \\
&\quad -\frac{1}{4}3\gamma_2 \cot^2\left(\frac{\sqrt{\gamma_2}(8\beta\gamma_2 t + x + y)}{\sqrt{2}}\right) - \frac{3\gamma_2}{2}, \\
\Psi_{30}(x,y,t) &= -\frac{1}{4}3\gamma_2 \tan^2\left(\frac{\sqrt{\gamma_2}(2\beta\gamma_2 t + x + y)}{\sqrt{2}}\right) - \frac{3\gamma_2}{4}, \\
\Psi_{31}(x,y,t) &= -\frac{1}{4}3\gamma_2 \cot^2\left(\frac{\sqrt{\gamma_2}(2\beta\gamma_2 t + x + y)}{\sqrt{2}}\right) - \frac{3\gamma_2}{4}, \\
\Psi_{32}(x,y,t) &= -\frac{1}{4}3\gamma_2 \tan^2\left(\frac{\sqrt{\gamma_2}(-2\beta\gamma_2 t + x + y)}{\sqrt{2}}\right) - \frac{\gamma_2}{4}, \\
\Psi_{33}(x,y,t) &= -\frac{1}{4}3\gamma_2 \cot^2\left(\frac{\sqrt{\gamma_2}(-2\beta\gamma_2 t + x + y)}{\sqrt{2}}\right) - \frac{\gamma_2}{4},
\end{aligned} \tag{29}$$

where the solution Ψ is equal to Γ in the corresponding cases and β is an arbitrary constant. In this discussion, we will cover the BS equation, which involves a constant known as β. These equations describe the interaction between a long wave along the $x-$axis and a Riemann wave that moves along the $y-$axis. α is used to represent the speed of the singularity. Figure 1 shows surface plots of the soliton solutions (a) $\Gamma_1(x,y,t)$ and (b) Γ_3 for $t = 0 \to 50$. Additionally, Figure 2 depicts the 3D wave profiles for the soliton solutions (a) Γ_5 and (b) Γ_{17} with $\beta = 1.2$ and $t = 0 \to 10$. The surface plots in the solution represent a brilliant-type wave profile.

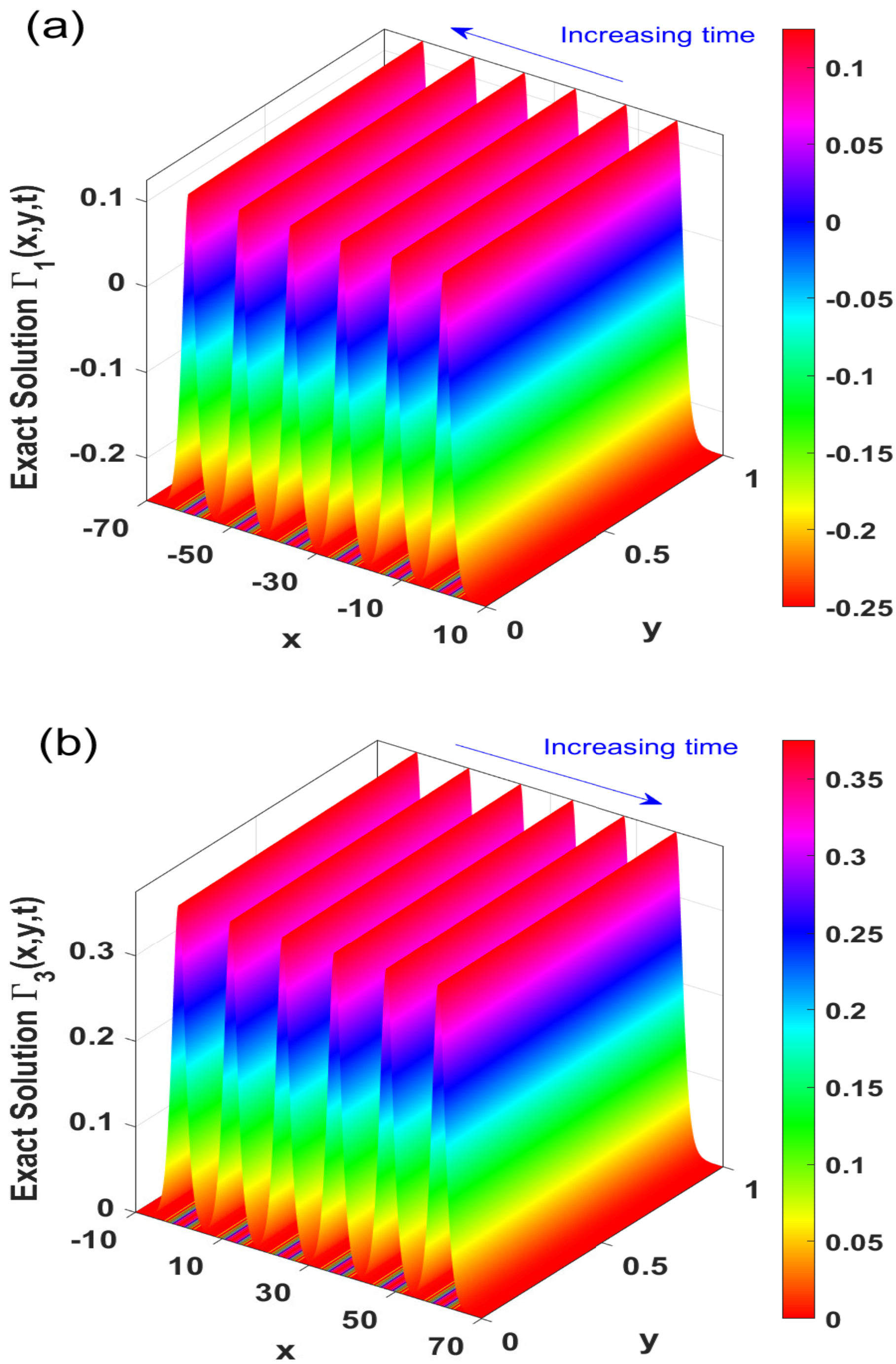

Figure 1. The time evolution of the exact solutions (**a**) Γ_1, and (**b**) Γ_3. The parameter is supplied by $\beta = 1.20$, with $t = 0 : 10 : 50$.

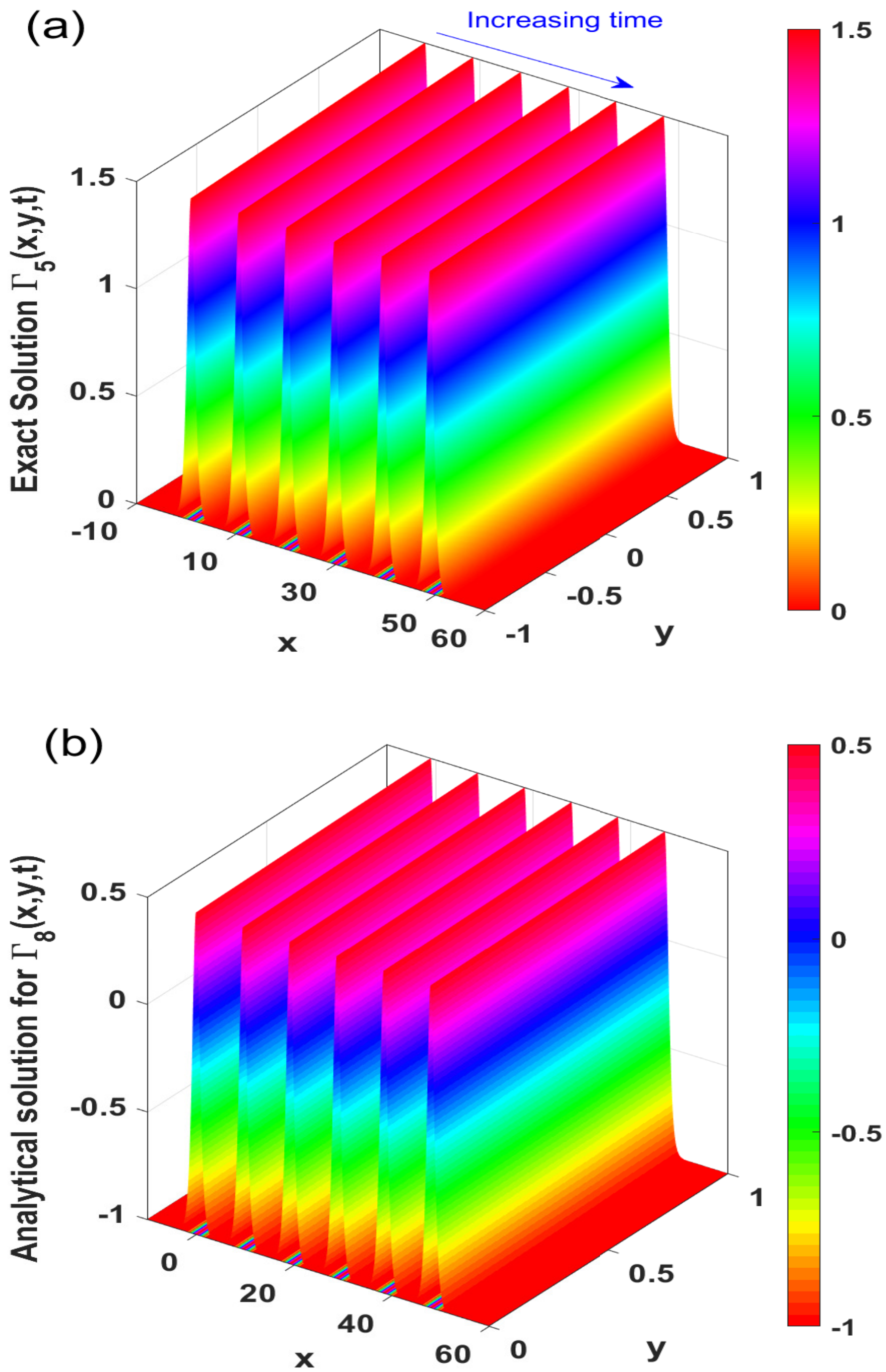

Figure 2. The time evolution of the exact solutions (**a**) Γ_5 and (**b**) Γ_{17}. The parameter is supplied by $\beta = 1.20$, with $t = 0:2:10$.

4. Numerical Solution

We employed various numerical techniques to ensure accurate analytical results when solving the ODEs (11). Using Γ_7 as an example, we set Φ and Θ to 0 at the endpoint where ζ is 0 and then guessed the starting values of Φ_ζ and Θ_ζ. At $t = 0$, we applied the nonlinear shooting and BVP methods to find the second $\Phi = 0$ boundary condition at a specific left endpoint of the domain. Once we obtain the numerical data, we compared them to the analytical solution Γ_7 at $t = 0$. We generated the numerical solution using FSOLVE and ODE15s in MATLAB [35]. The discretized version of the resulting ODE (11), which is

$$-\alpha\,\Phi + 2\beta\,\Theta^2 + 2\beta\,\Phi^2 + \frac{\beta}{\delta\zeta^2}\,(\Phi_{i+1} - 2\Phi_i + \Phi_{i-1}) = 0, \tag{30}$$

was subjected to the shooting method. Figure 3 displays a comparison of the analytic and numerical solutions obtained using the aforementioned numerical approaches, all of which were identical. The accuracy of the analytical solution could, therefore, be checked using this method. The acquired numerical solution can serve as an initial condition for the numerical scheme discussed in the following section.

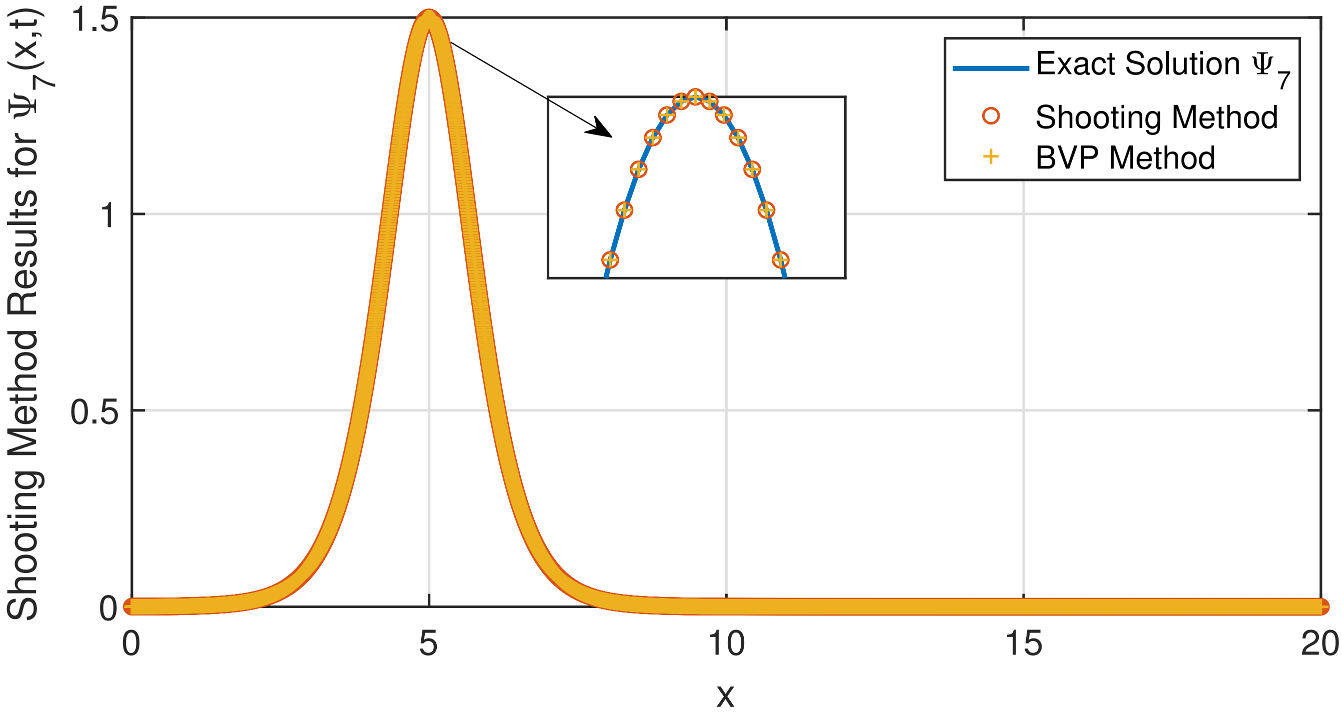

Figure 3. Comparison of Γ_7 at $t = 0$ via analytical and numerical methods. With parameters $\beta = 1.2$, $x = 0 \to 20$, and $N = 3200$.

To calculate the numerical outcomes of System (1) within the rectangular domain $[a, b] \times [0, 1]$, I will be using the finite differences method. The starting point and ending point of the rectangle along the $x-$axis are represented by a and b, respectively. The rectangular area enclosed by $[a, b] \times [0, 1]$ is divided into $(N+1) \times (J+1)$ mesh points. These points are arranged as

$$\begin{aligned} x_i =& a + i\,\Delta x, \qquad i = 0, 1, 2, \ldots, N, \\ y_j =& j\,\Delta y, \qquad j = 0, 1, 2, \ldots, J, \end{aligned}$$

where Δx and Δy are the x *and* y domain step sizes, respectively. System (1) is turned into an ODE system by discretizing the space derivatives while keeping the time derivative continuous. Completing this process yields the desired results.

$$\begin{aligned} \Gamma_t|_{i,j}^n =& -\frac{2\beta}{\Delta x}\left[\Gamma^{n+1}_{i+\frac{1}{2},j}(\Psi^{n+1}_{i+1,j} - \Psi^{n+1}_{i-1,j}) + \Psi^{n+1}_{i+\frac{1}{2},j}(\Gamma^{n+1}_{i+1,j} - \Gamma^{n+1}_{i-1,j})\right] \\ & - \frac{\beta}{2\Delta y}\delta_x^2(\Gamma^{n+1}_{i,j+1} - \Gamma^{n+1}_{i,j-1}), \\ 0 =& \frac{1}{2\Delta x}(\Psi^{n+1}_{i+1,j} - \Psi^{n+1}_{i-1,j}) - \frac{1}{2\Delta y}(\Gamma^{n+1}_{i,j+1} - \Gamma^{n+1}_{i,j-1}), \end{aligned} \tag{31}$$

where

$$\delta_x^2 \Gamma_{i,j}^{n+1} = \left(\Gamma_{i+1,j}^{n+1} - 2\Gamma_{i,j}^{n+1} + \Gamma_{i-1,j}^{n+1} \right).$$

According to the boundary conditions

$$\begin{aligned} \Gamma_x(a,\, y,\, t) &= \Gamma_x(b,\, y,\, t) = 0, \quad \forall y, \\ \Gamma_y(x,\, 0,\, t) &= \Gamma_y(x,\, 1,\, t) = 0, \quad \forall x, \end{aligned} \tag{32}$$

The boundary constraints enabled us to evaluate the space derivatives at the domain's endpoints using fictitious points. The following factors contributed to the initial conditions:

$$\Gamma_{10}(x, y, t = 0) = \frac{3}{2}\gamma_2 \,\mathrm{sech}^2(\sqrt{\gamma_2}(x + y + x0)), \tag{33}$$

where $\gamma_2 > 0$ is the setting chosen by the user. The parameter values are held constant throughout all of the numerical results presented in this section as $\beta = 0.1$, $x0 = -5.0$, $y = 0 \to 1$, $x = 0 \to 20$ and $t = 0 \to 25$. It is important to note that we utilized the DDASPK solver [36], a FORTRAN software 95 that effectively solves ODEs, to solve System (31). The solver employed a regressive differentiation formula that necessitated an LU-factorization approximation of the Jacobian matrix of the linearized system, as there was no initial condition for the space derivatives. The numerical outcomes we acquired are satisfactory, and the figures below demonstrate their comprehension.

5. Stability of the Numerical Scheme

The stability of the numerical solution was investigated using the Fourier stability technique. This technique employs Fourier analysis, also known as von Neumann analysis, to assess the stability of the scheme (31). It is important to note that this method is only suitable for situations that involve linear equations. Therefore, the goal was to transform the given equations linearly.

$$\begin{aligned} &\Gamma_t + 4\beta\Gamma\,\Psi_x + 4\beta\Gamma_x\,\Psi + \beta\,\Gamma_{xxy} = 0, \\ &\Psi_x - \Gamma_y = 0. \end{aligned} \tag{34}$$

By examining the second equation of System (34), it can be observed that Γ is equal to Ψ. Hence, the first equation in (34) can be expressed as

$$\Gamma_t + 8\beta\,\Gamma\,\Gamma_x + \beta\,\Gamma_{xxy} = 0. \tag{35}$$

where β is a constant. In order to employ the Fourier stability approach, it is important to possess linear equations. Hence, in order to align Equation (35) with this approach, it is necessary to convert it into a linear equation.

$$\Gamma_t + d_0\Gamma_x + \beta\,\Gamma_{xxy} = 0, \tag{36}$$

where $d_0 = 8\beta\,\Gamma$ is quantized and held constant by

$$d_0 = \max_{\substack{1 \le i \le N \\ 1 \le j \le J}} \left(8\beta\,\Gamma_{i,j}^n \right).$$

Equation (36) can be expressed using the finite difference method.

$$\begin{aligned} \Gamma_{i,j}^n = &\Gamma_{i,j}^{n+1} + D_1\Gamma_{i+1,j}^{n+1} - D_1\Gamma_{i-1,j}^{n+1} + D_2\left(\Gamma_{i+1,j+1}^{n+1} - 2\Gamma_{i,j+1}^{n+1} + \Gamma_{i-1,j+1}^{n+1} \right) \\ &- D_2\left(\Gamma_{i+1,j-1}^{n+1} - 2\Gamma_{i,j-1}^{n+1} + \Gamma_{i-1,j-1}^{n+1} \right), \end{aligned} \tag{37}$$

where $D_1 = 0.5\frac{d_0 \Delta t}{\Delta x}$, $D_2 = 0.5\frac{\beta \Delta t}{\Delta y}$. It is essential to consider the boundary conditions as neglecting them can lead to significant consequences. Assume that $x_i = i\Delta x, y_j = j\Delta y$ and $t_n = n\Delta t$; then,

$$\begin{gathered} \Gamma_{i,j}^{n} = \mu^{n} e^{\iota \xi \pi i \Delta x} e^{\iota \eta \pi j \Delta y} \quad \text{and then} \quad \Gamma_{i,j}^{n+1} = \mu \Gamma_{i,j}^{n}, \\ i = 1,2,3,\ldots,N, \quad j = 1,2,3,\ldots,M \text{ and } \forall n. \end{gathered} \tag{38}$$

By substituting (38) into (36), we obtain the subsequent results:

$$\Gamma_{i,j}^{n} = \mu \Gamma_{i,j}^{n} + 2D_1 \sin(\Delta x \xi \pi) \mu \Gamma_{i,j}^{n} - 8iD_2 \sin^2\left(\frac{\Delta x \xi \pi}{2}\right) \sin(\eta \pi \Delta y) \mu \Gamma_{i,j}^{n}. \tag{39}$$

Thus,

$$\mu = \frac{1}{\left(1 + 2D_1 \sin(\xi \pi \Delta x) - 8iD_2 \sin^2\left(\frac{\Delta x \xi \pi}{2}\right) \sin(\Delta y \eta \pi)\right)}. \tag{40}$$

Let

$$v = 2D_1 \sin(\Delta x \xi \pi) - 8iD_2 \sin^2\left(\frac{\Delta x \xi \pi}{2}\right) \sin(\Delta y \eta \pi). \tag{41}$$

Equation (40) can be rewritten as:

$$|\mu| = \left| \frac{1}{1+v} \right| \leq 1. \tag{42}$$

Based on our comprehensive study, we can assert with confidence that the scheme under consideration exhibits stability and adheres to the established norms of Fourier stability. Maintaining a value of mu below one is crucial, and we can verify that our system successfully meets this criterion. The equation shown in (40) provides clear evidence that the absolute value of μ is less than one, ensuring the stability of our numerical system under all circumstances.

6. Error Analysis

To determine the accuracy order of Scheme (31), I utilized the Taylor series. The order was calculated based on the evaluation of the truncation error. Here, we assume that

$$e_{i,j}^{n+1} = \Gamma_{i,j}^{n+1} - \Gamma(x_i, y_j, t_{n+1}). \tag{43}$$

In order to study the error analysis at a specific position and time (x_i, y_j, t_{n+1}), we utilize $e_{i,j}^{n+1}$, which denotes the error. The estimated solution is referred to as $\Gamma_{i,j}^{n}$, while the analytical solution is $\Gamma(x_i, y_j, t_{n+1})$. The ultimate outcome can be achieved by incorporating (43) into scheme (37).

$$\begin{aligned} e_{i,j}^{n} = & e_{i,j}^{n+1} + D_0 e_{i+1,j}^{n+1} - D_0 e_{i-1,j}^{n+1} + D_1\left(e_{i+1,j+1}^{n+1} - 2e_{i,j+1}^{n+1} + e_{i-1,j+1}^{n+1}\right) \\ & - D_1\left(e_{i+1,j-1}^{n+1} - 2e_{i,j-1}^{n+1} + e_{i-1,j-1}^{n+1}\right) - \Delta t T_{i,j}^{n}, \end{aligned} \tag{44}$$

where $D_0 = \frac{d_0 \Delta t}{2\Delta x}$ and $D_1 = \frac{\beta \Delta t}{2\Delta y}$. In addition, $T_{i,j}^{n}$ presents a way to express the truncation error, which is as follows:

$$\begin{aligned} T_{i,j}^{n} = & \Gamma(x_i, y_j, t_{n+1}) + D_0 \Gamma(x_{i+1}, y_j, t_{n+1}) - D_0 \Gamma(x_{i-1}, y_j, t_{n+1}) \\ & + D_1\left(\Gamma(x_{i+1}, y_{j+1}, t_{n+1}) - 2\Gamma(x_i, y_{j+1}, t_{n+1}) + \Gamma(x_{i-1}, y_{j+1}, t_{n+1})\right) \\ & - D_1\left(\Gamma(x_{i+1}, y_{j-1}, t_{n+1}) - 2\Gamma(x_i, y_{j-1}, t_{n+1}) + \Gamma(x_{i-1}, y_{j-1}, t_{n+1})\right), \end{aligned} \tag{45}$$

Hence,

$$T_{i,j}^n \leq \frac{\Delta t}{2}\Gamma_{tt}(x_i, y_j, \eta0_{n+1}) - \frac{\Delta x \Delta y}{4}\Gamma_{xxxyy}(\eta1_i, \eta2_j, t_{n+1}) - \frac{\Delta x^2}{6}\Gamma_{xxx}(\eta1_i, y_j, t_{n+1}), \quad (46)$$

where $\eta0_{n+1} \in (t_n, t_{n+1})$, $\eta1_i \in (x_{i-1}, x_{i+1})$, and $\eta2_j \in \left(y_{j-1}, y_{j+1}\right)$. Thus, the numerical scheme's truncation error is $T_{i,j}^n = O(\Delta t) + O(\Delta y^2) + O(\Delta x^2)$. Consequently, every step's truncation error is indicated by

$$T_{i,j}^n = O\left(\Delta t, \Delta y^2, \Delta x^2\right).$$

Performing a series of computations using the initial data and refining it with distinct meshes, gives (Δx, Δy, $\Delta t \to 0$).

7. Convergence of the Numerical Schemes

In order to determine whether a numerical scheme is convergent within a specific domain D, the first step is to evaluate each fixed point $(x^*, y^*, t^*) \in D$. If $(x_i, y_j, t_n) \to (x^*, y^*, t^*)$, then $\Gamma_{i,j}^n = \Gamma(x^*, y^*, t^*)$ and the numerical scheme is convergent. Earlier, I demonstrated that the implicit scheme guarantees the unconditional stability of the system. In order to confirm that its convergence is unconditional, let us assume that the mistake is represented by e, which is made possible by

$$e_{i,j}^n = \Gamma_{i,j}^n - \Gamma(x_i, y_j, t_n). \quad (47)$$

Despite the truncation error indication, $\Gamma_{i,j}^n$ removes it and successfully fulfilled the strategy outlined in Equation (31). Thus,

$$\begin{aligned} e_{i,j}^n =& e_{i,j}^{n+1} + D_1 e_{i+1,j}^{n+1} - D_1 e_{i-1,j}^{n+1} + D_2\left(e_{i+1,j+1}^{n+1} - 2e_{i,j+1}^{n+1} + e_{i-1,j+1}^{n+1}\right) \\ &- D_2\left(e_{i+1,j-1}^{n+1} - 2e_{i,j-1}^{n+1} + e_{i-1,j-1}^{n+1}\right) - \Delta t T_{i,j}^n, \end{aligned} \quad (48)$$

where $D_1 = 0.5\frac{d_0 \Delta t}{\Delta x}$, $D_2 = 0.5\frac{\beta \Delta t}{\Delta y}$. Assuming that the following is the correct way to define the maximum error for each time step:

$$E^n = \max\left\{\left|e_{i,j}^n\right|, \forall i, j \text{ and } n \geq 0\right\}. \quad (49)$$

Consequently, the result of implementing Equation (49) within Equation (48) is

$$e_{i,j}^{n+1} \leq E^n + \Delta t T_{i,j}^n, \quad (50)$$

Subsequently, for every value of $i = 1, \ldots, N$, $j = 1, \ldots, M$ gives

$$E^{n+1} \leq E^n + \Delta t T_{i,j}^n. \quad (51)$$

Based on the original data, it is possible to determine that $E^0 = 0$. Therefore, the inequality is expressed as

$$E^1 \leq E^0 + \Delta t T_{i,j}^n = \Delta t T_{i,j}^n \quad \Rightarrow \quad E^2 \leq E^1 + \Delta t T_{i,j}^n \leq 2\Delta t T_{i,j}^n.$$

Thus, we have

$$E^n \leq n \times \Delta t T_{i,j}^n. \quad (52)$$

When Δx, Δy, $\Delta t \to 0$, the value of $T_{i,j}^n \to 0$; hence,

$$E^k \leq k \times \Delta t T_{n,m}^k \to 0 \qquad \text{as} \qquad \Delta t \to 0. \quad (53)$$

Therefore, it may be concluded that the scheme (Equation (31)) exhibits convergence when $\Delta x, \Delta y, \Delta t \to 0$.

8. Result and Discussion

This study focuses on the significant outcomes and methods employed. The exact solutions for Equation (1) can be obtained using the generalized indirect algebraic and modified $S-$expansion methods. Figures 1, 2 and 4 display some solitary wave solutions for the parameters $\beta = 1.20$, $N = 100$, and $M = 3200$, respectively. I also used a numerical scheme (31) to confirm these solutions and obtain numerical results. Figure 5 and Table 3 present the main findings, facilitating the comparison between the analytical and numerical solutions. Based on the above analysis, it is evident that the solutions exhibit a high degree of similarity, and the error significantly diminishes as Δx and Δy approach zero. Any value of parameter β must remain unchanged for the numerical schemes to maintain stability. Any alteration to this parameter may lead to instability and should be avoided at all costs. Figure 1a,b present the time evolution of the analytic solutions (a) Γ_1 with $x = -70 \to 10$ and (b) Γ_3 with $x = -10 \to 70$. These figures are plotted at $t = 0 \to 50$ and $\beta = 1.2$. The firing method efficiently addresses the stated problem. Figure 2a,b present the time evolution of the analytic solutions (a) Γ_5 with $x = -10 \to 60$ and (b) Γ_8 with $x = -10 \to 60$. These figures are plotted at $t = 0 \to 10$ and $\beta = 1.2$. Figure 4a,b present the time evolution of the analytic solutions (a) Γ_{11} with $x = -1 \to 1$ and (b) Γ_{17} with $x = -10 \to 60$. These figures are plotted at $t = 0 \to 10$, and $\beta = 1.2$. To create the numerical results of Equation (31), the solution was used as an initial condition for the numerical scheme. Figure 6 shows the exact solution for a single traveling wave and the shooting method solutions. These solutions are mutually conducive and behave as a unit, indicating that the methods employed are valid and successful. The Taylor series expansion was also used to examine the scheme's precision. The precision was determined beginning with the second order. The proposed numerical technique is only approximately accurate to the second order, as indicated in Figure 5. The Von Neumann analysis demonstrates the unconditional stability of the numerical system.

Figure 7a,b depict the time progression of the exact and numerical results with $\beta = 0.1$, $x0 = -5.0$, $y = 0 \to 1$, $x = 0 \to 20$, $t = 0 \to 25$, $J = 100$, and $N = 3200$. It can be seen that the constructed accurate traveling solutions match with the numerical solutions. The resulting accurate solitary traveling wave and numerical solutions at $t = 25$ are displayed in $3D$ in Figure 8a,b. These graphs make it clear that the exact solutions exhibit behaviors similar to those of the numerical solutions. Table 3 and Figure 5 also demonstrate the efficacy of the techniques employed. The $L2$ error and the amount of CPU time needed to arrive to time step 5 using the numerical scheme are shown in Table 3. Increasing the number of points dramatically reduces inaccuracy and increases the CPU time required to process them. The finite difference method is more suitable for solving nonlinear partial differential equations computationally because it provides the high-error locations with sufficient data points, quickly decreasing the error.

Table 3. The relative error formula RLTV is used here to measure the error with fixing $\Delta t = 1 \times 10^{-2}$ at a specific time $t = 25$.

Δx	RLTV	CPU
1.0×10^{-1}	1.5×10^{-3}	56.0 s
5.0×10^{-2}	3.2×10^{-4}	133.36 s
2.5×10^{-2}	1.6×10^{-4}	316.20 s
1.25×10^{-2}	4.4×10^{-5}	619.80 s
6.3×10^{-3}	1.2×10^{-5}	1492.86 s

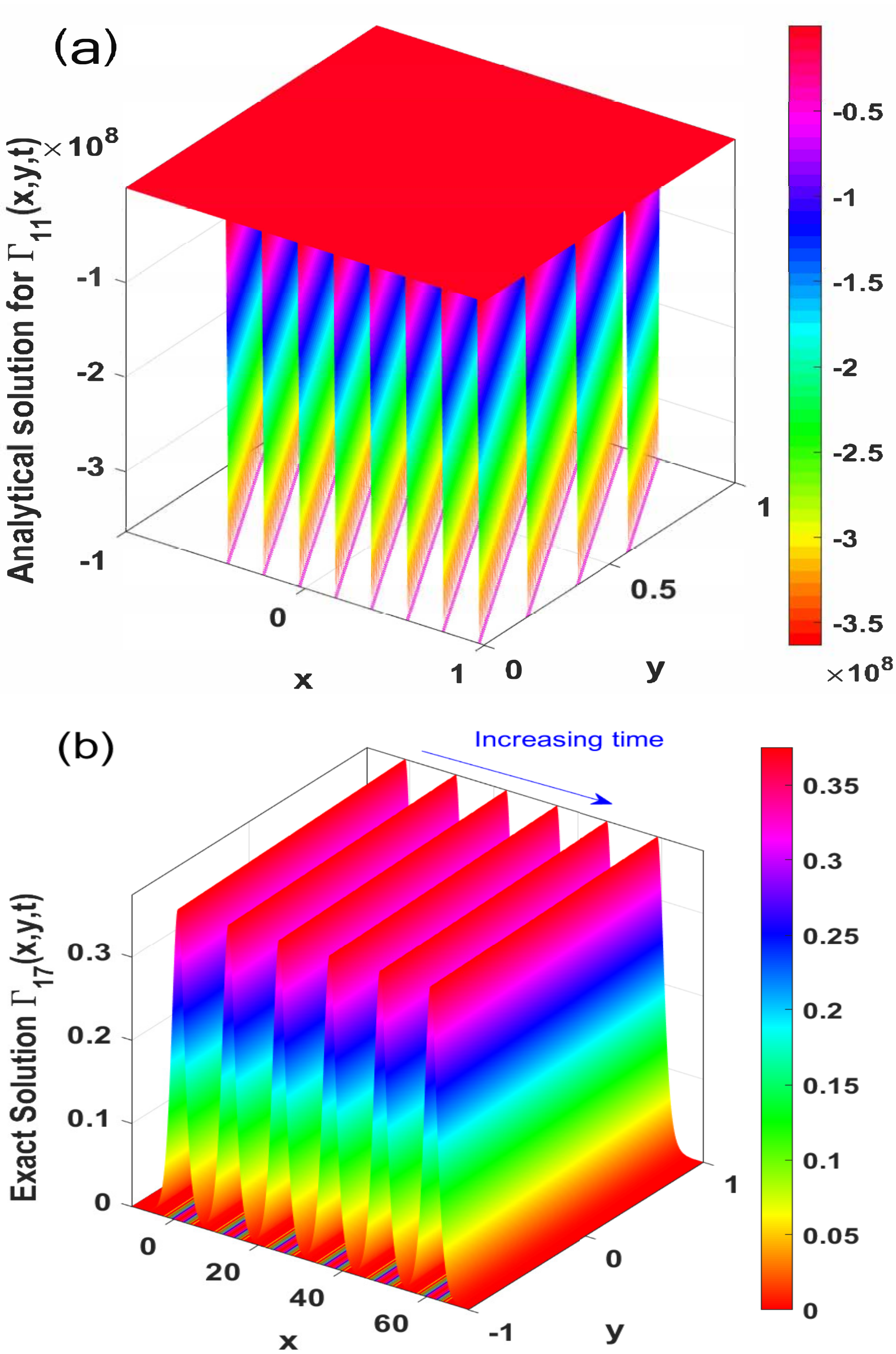

Figure 4. The time evolution of the exact solutions (**a**) Γ_5 and (**b**) Γ_{17}. The parameter is supplied by $\beta = 1.20$, with $t = 0 : 2 : 10$.

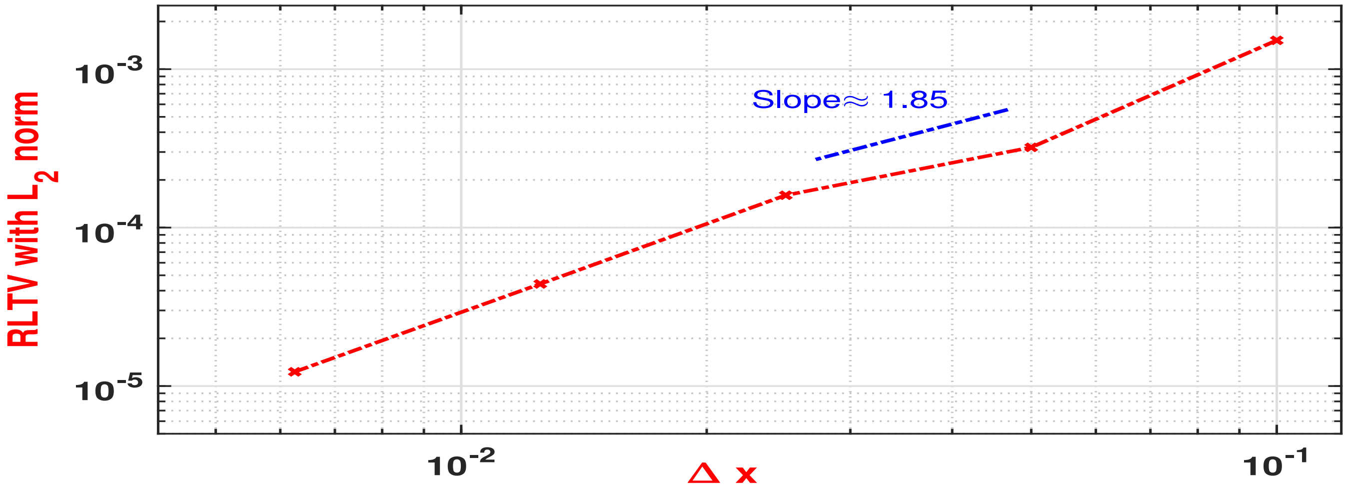

Figure 5. The convergence records based on Δx utilizing the l_2 norm relative error from Table 3). As for the variable y, the value of 0.5 at $t = 25$ and $x = 0 \rightarrow 20$ was specifically selected.

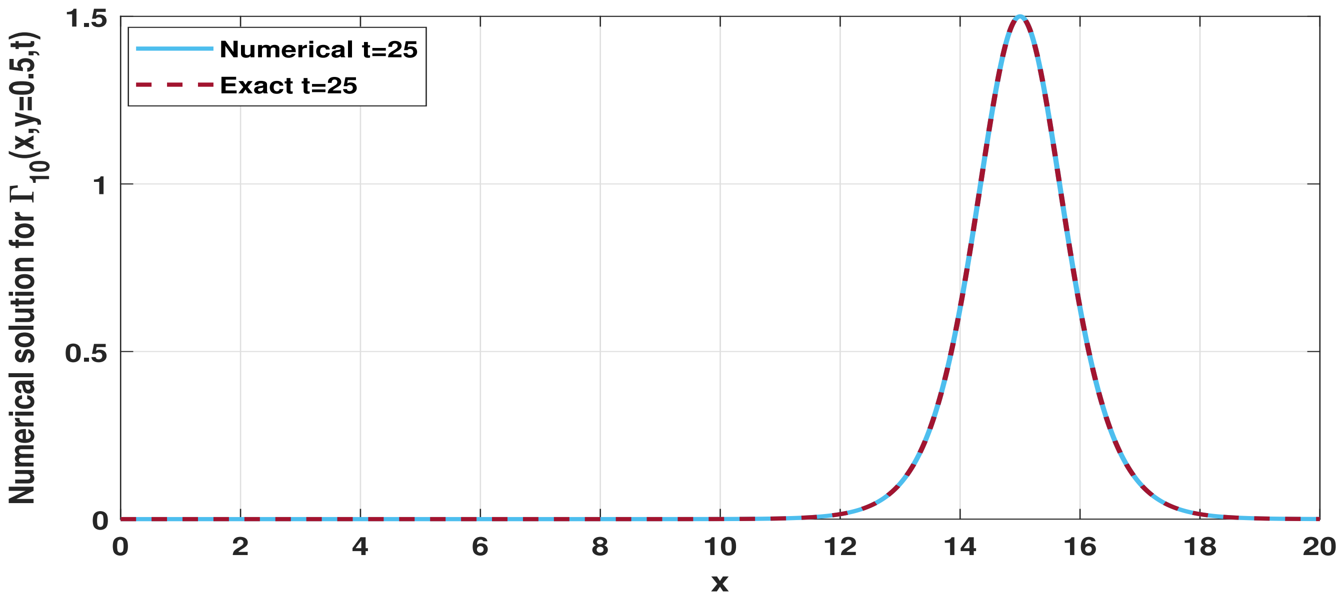

Figure 6. Change in the time frame for the numerical results. Maintaining the constant values of $y = 0.5$ at $t = 25$ is crucial. Upon close observation of the wave, it is clear that there is a close resemblance between the numerical and analytic solutions.The parameter values are determined by $\beta = 0.1$, $x0 = -5.0$, $x = 0 \rightarrow 20$, $t = 0 \rightarrow 25$, $J = 100$, and $N = 3200$.

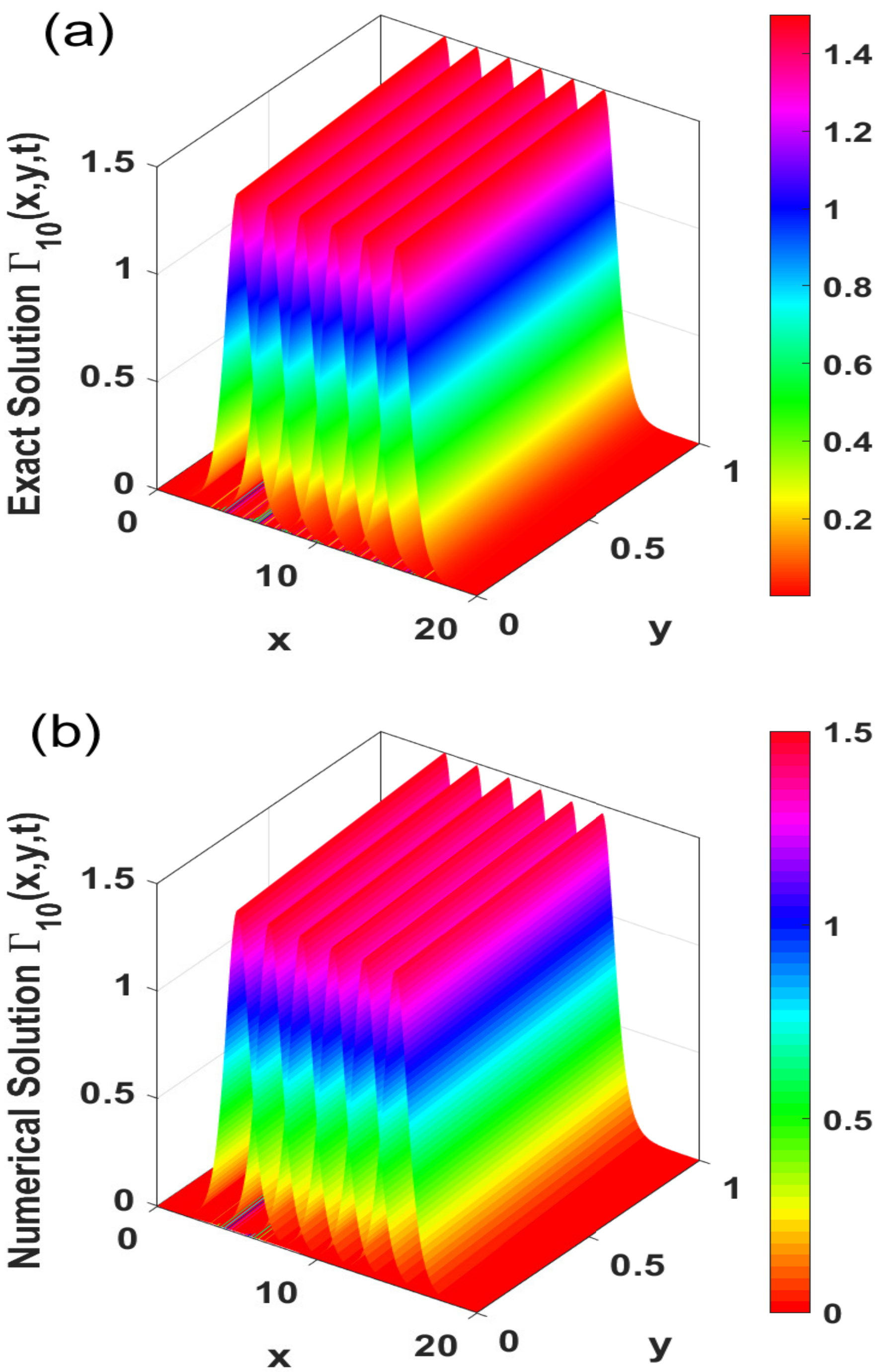

Figure 7. The analytical (**a**) and numerical (**b**) solutions for Γ_{10} are shown in 3D. The parameter values are determined by $\beta = 0.1$, $x0 = -5.0$, $y = 0 \rightarrow 1$, $x = 0 \rightarrow 20$, $t = 0 \rightarrow 25$, $J = 100$, and $N = 3200$.

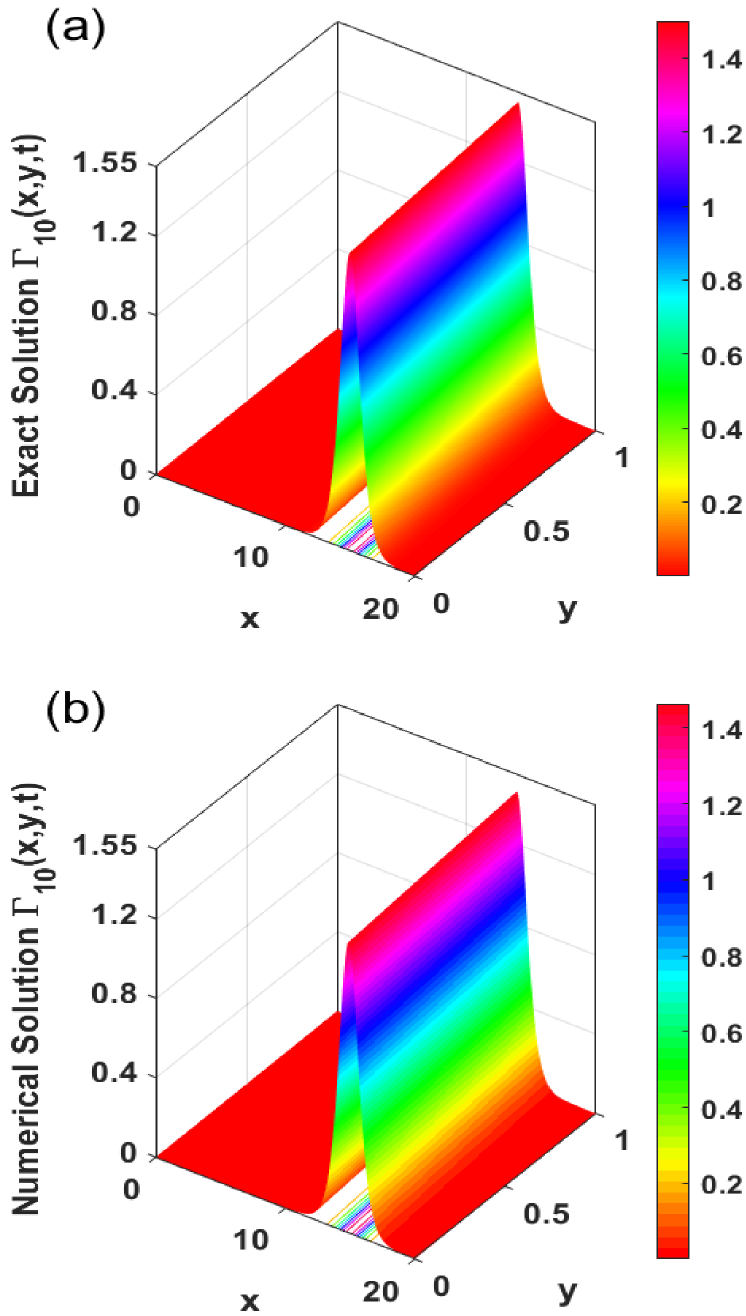

Figure 8. The resulting (**a**) accurate solitary traveling wave and (**b**) numerical solutions at $t = 25$ with $\beta = 1.2$, $x = 0 \to 20$, $y = 0 \to 1$, $N = 3200$, and $J = 100$.

9. Conclusions

In this study, we used the generalized indirect algebraic and modified S-expansion methods to derive various types of solitary wave solutions for the BS equations. These solutions were presented in the form of hyperbolic and trigonometric functions. To solve the suggested problem, we used the shooting method to construct a solution, which we then used as an initial condition for a numerical scheme. The numerical solution to the problem was achieved successfully without any issues. We conducted an in-depth analysis of the differences and similarities between the analytical and numerical results to validate the constructed solutions. The solutions behaved almost identically to one another. The finite differences approach achieved a significantly higher accuracy, contributing to the method's significant improvement. We determined that the numerical scheme is unconditionally stable, and there is a correlation between the total number of points and the relative error. From a computational standpoint, the methods utilized are effective.

Funding: The authors extend their appreciation to the Deanship of Research and Innovation at the Ministry of Education in Saudi Arabia for funding this research through project number 445-9-535.

Data Availability Statement: The datasets generated during and/or analyzed during the current study are available from the corresponding author on reasonable request.

Conflicts of Interest: The author declares that he has no potential conflicts of interest.

References

1. Akbulut, A.; Islam, S.; Rezazadeh, H.; Tascan, F. Obtaining exact solutions of nonlinear partial differential equations via two different methods. *Int. J. Mod. Phys. B* **2022**, *36*, 2250041. [CrossRef]
2. Wen-Xiu, M.; Yong, X.; Zhang, H. Diversity of interaction solutions to the (2+1)-dimensional Ito equation. *Comput. Math. Appl.* **2018**, *75*, 289–295. [CrossRef]
3. Ozkam, Y.; Yasar, E.; Osman, M. Novel multiple soliton and front wave solutions for the 3D-Vakhnenko–Parkes equation. *Mod. Phys. Lett. B* **2022**, *36*, 2250003. [CrossRef]
4. Bashar, M.; Islam, S. Exact solutions to the (2 + 1)-Dimensional Heisenberg ferromagnetic spin chain equation by using modified simple equation and improve F-expansion methods. *Phys. Open* **2020**, *5*, 100027. [CrossRef]
5. Zaki, S. Solitary wave interactions for the modified equal width equation. *Comput. Phys Commun.* **2000**, *126*, 219–231. [CrossRef]
6. Wazwaz, A. The tanh method and the sine–cosine method for solving the KP-MEW equation. *Int. J. Comput. Math.* **2005**, *82*, 235–246. [CrossRef]
7. Alharbi, A.; Faisal, M.; Shah, F.; Waseem, M.; Ullah, R. ; Sherbaz, S. Higher Order Numerical Approaches for Nonlinear Equations by Decomposition Technique. *IEEE Access* **2019**, *7*, 44329–44337. [CrossRef]
8. Radha, R.; Lakshmanan, M. Dromion like structures in the (2 + 1)-dimensional breaking soliton equation. *Phys. Lett. A* **1995**, *197*, 7–12. [CrossRef]
9. Yan, Z.; Zhang, H. Constructing families of soliton-like solutions to a (2+1)-dimensional breaking soliton equation using symbolic computation. *Int. J. Comput. Math. Appls.* **2002**, *44*, 1439–1444. [CrossRef]
10. Chen, Y.; Biao, L.; Zhang, H. Symbolic Computation and Construction of Soliton-Like Solutions to the (2+1)-Dimensional Breaking Soliton Equation. *Commun. Theor. Phys.* **2003**, *40*, 137–142. [CrossRef]
11. Peng, Y.; Krishnan, E. Two Classes of New Exact Solutions to (2+1)-Dimensional Breaking Soliton Equation. *Commun. Theor. Phys.* **2005**, *44*, 807–809. [CrossRef]
12. Inan, I. Generalized Jacobi Elliptic Function Method for Traveling Wave Solutions of (2+1)-Dimensional Breaking Soliton Equation. *Cankaya Univ. J. Sci. Eng.* **2010**, *7*, 39–50.
13. Cheng, W.; Chen, Y. Nonlocal symmetry and exact solutions of the (2+1)- dimensional breaking soliton equation. *Commun. Nonlinear Sci. Numer. Simulat.* **2015**, *29*, 198–207. [CrossRef]
14. Osman, M.S. On multi-soliton solutions for the (2+1)-dimensional breaking soliton equation with variable coefficients in a graded-index waveguide. *Comput. Math. Appls.* **2018**, *75*, 1–6. [CrossRef]
15. Manafian, J.; Behnam, M.; Abapour, M. Lump-type solutions and interaction phenomenon to the (2+1)-dimensional Breaking Soliton equation. *Appl. Math. Comput.* **2019**, *356*, 13–41. [CrossRef]
16. Kumar, M.; Tanwar, D. Lie symmetries and invariant solutions of $(2+1)$-dimensional breaking soliton equation. *Pranama J. Phys.* **2020**, *94*, 23. [CrossRef]
17. Baskonus, H.; Kumar, A.; Wei, G. Deeper investigations of the (4 + 1)-dimensional Fokas and (2 + 1)-dimensional Breaking soliton equations. *Int. J. Mod. Phys. B* **2020**, *34*, 2050152. [CrossRef]
18. Alharbi, A. Numerical solutions to two-dimensional fourth order parabolic thin film equations using the Parabolic Monge-Ampere method. *AIMS Math.* **2023**, *8*, 16463–16478. [CrossRef]
19. Ren, B.; Chu, P. Dynamics of D'Alembert wave and soliton molecule for a (2+1)-dimensional generalized breaking soliton equation. *Chin. J. Phys.* **2021**, *74*, 296–301. [CrossRef]
20. Kaplan, M.; Akbulut, A. The analysis of the soliton-type solutions of conformable equations by using generalized Kudryashov method. *Opt. Quantum. Electron.* **2021**, *53*, 498. [CrossRef]
21. Qin, Y.; Gao, Y.; Shen, Y.; Sun, Y.; Meng, G.; Yu, X. Solitonic interaction of a variable coefficient (2 + 1)-dimensional generalized Breaking Soliton equation. *Phys. Scr.* **2013**, *88*, 1–7. [CrossRef]
22. Mirzazadeh, M.; Hosseini, K.; Dehingia, K.; Salahshour, S. A second-order nonlinear Schrödinger equation with weakly nonlocal and parabolic laws and its optical solitons. *Optic* **2021**, *242*, 166911. [CrossRef]
23. Xia, T.; Xiong, S. Exact solutions of (2 + 1)-dimensional Bogoyavlenskii's Breaking Soliton equation with symbolic computation. *Comput. Math. Appl.* **2010**, *60*, 919–923. [CrossRef]
24. Alharbi, A.; Almatrafi, M.; Abdelrahman, M. Analytical and numerical investigation for Kadomtsev–Petviashvili equation arising in plasma physics. *Phys. Scr.* **2020**, *95*, 045215. [CrossRef]

25. Alharbi, A. A Study of Traveling Wave Structures and Numerical Investigation of Two-Dimensional Riemann Problems with Their Stability and Accuracy. *Comput. Model. Eng. Sci.* **2023**, *134*, 2193–2209. [CrossRef]
26. Cao, L.; Wang, D.; Chen, L. Symbolic computation and q-deformed function solutions of (2 + 1)-dimensional Breaking Soliton equation. *Commun. Theor. Phys.* **2007**, *47*, 270–274. [CrossRef]
27. Zhang, S. A generalized new auxiliary equation method and its application to the (2 + 1)-dimensional Breaking Soliton equations. *Appl. Math. Comput.* **2007**, *190*, 510–516. [CrossRef]
28. Bogoyavlensky, O. Overturning solitons in new two-dimensional integrable equations. *Izv. Akad. Nauk SSSR Ser. Mat.* **1989**, *53*, 243–257. [CrossRef]
29. Calogero, F.; Degasperis, A. Nonlinear evolution equations solvable by the inverse spectral transform—I. *Il Nuovo Cimento B* **1976**, *32*, 201–242. [CrossRef]
30. Calogero, F.; Degasperis, A. Nonlinear evolution equations solvable by the inverse spectral transform— II. *Il Nuovo Cimento B* **1977**, *39*, 1–54. [CrossRef]
31. Kazeykina, A.; Klein, C. Numerical study of blow-up and stability of line solitons for the Novikov- Veselov equation. *Nonlinearity* **2017**, *30*, 2566. [CrossRef]
32. Sagar, B.; Saha, S. Numerical soliton solutions of fractional (2+1)-dimensional Nizhnik-Novikov-Veselov equations in nonlinear optics. *Int. J. Mod. Phys. B* **2021**, *35*, 2150090. [CrossRef]
33. Bai, C.; Bai, C.; Zhao, H. A new generalized algebraic method and its application in nonlinear evolution equations with variable coefficients. *Z. Naturforsch. A* **2005**, *60*, 211–220. [CrossRef]
34. Aasaraai, A. The application of modified F-expansion method solving the Maccari's system. *J. Adv. Math. Comput. Sci.* **2015**, *11*, 1–14. [CrossRef]
35. Shampine, L.; Reichelt, M. The matlab ode suite. *SIAM J. Sci. Comput.* **1994**, *18*, 1–22. [CrossRef]
36. Brown, P.; Hindmarsh, A.; Petzold, L.E. Using Krylov methods in the solution of large-scale differential-algebraic systems. *SIAM J. Sci. Comput.* **1994**, *15*, 1467–1488. [CrossRef]